

An Inverse Transport Approach to Radiation Source Location for Border Security

Karen A. Miller, William S. Charlton

Texas A&M University
Nuclear Engineering Department
College Station, TX 77843-3133 USA
E-mail: karen_miller@tamu.edu, wcharlton@tamu.edu

Abstract:

Radiation portal monitors are being deployed at border crossings throughout the world to help prevent against the smuggling of nuclear and radiological materials. Many of these borders have several lanes for vehicles, each equipped with a portal monitor. With the current technology, if the detectors are alarmed, border guards must stop traffic and search for the source. In some cases, it can take hours to get through a busy border crossing. If radiation detection equipment adds a mere twenty seconds per car, this wait can increase by more than an hour. Another problem with these systems derives from the fact that one source can set off detectors in multiple lanes. If the source is being shielded by a vehicle in its lane, it may set off detectors in adjacent lanes but not its own.

The purpose of this research is to develop an algorithm for identifying the location of a radioactive source using a distributed array of detectors. To locate the source, some knowledge about the vehicles is needed. When a detector is alarmed, cameras installed in each lane will take a picture of the vehicles and a computer algorithm will build a cross section model of the traffic. The cross section model will be used in neutron and radiation transport calculations to determine the position of the radioactive material. There has been a lot of work done using inverse transport calculations to determine the material properties of an object, and this work uses some of the same techniques for source location. Forward transport calculations using a step-difference approximation are used to define an error functional describing the difference between the actual and calculated detector readings given an estimated source location. Adjoint transport calculations making use of a steepest descent method are used to minimize that error functional and thus identify the source location.

Keywords: border; smuggling; inverse; transport; adjoint

1. Introduction

The United States Department of Homeland Security (DHS) has been deploying radiation detection equipment to the nation's border sites. One of the goals of this program is to screen all of the traffic coming into the U.S. without causing delays. The U.S. has over 380 ports-of-entry, and each day the DHS processes approximately 365,000 vehicles and over 1.1 million people arriving in the country. At the San Ysidro, California land border crossing it was estimated that prior to the installment of portal monitors it would take about 2.5 hours to get through the border at peak times. If the radiation detection equipment adds a mere 20 seconds for each vehicle this wait increases to 3.5 to 4 hours¹.

Many of these ports-of-entry have several lanes for vehicles, each equipped with a portal monitor. If a vehicle contains radioactive material, it may set off one or more of the detectors. Once detectors are alarmed Customs and Border Protection agents must stop traffic, locate the source, and identify the nature of the material. Not only is this inspection process time-consuming, there is also the threat that a source can set off detectors in adjacent lanes and not set off detectors in its own lane. If this happens, the source may get through the border. This underlines the need for a faster and more accurate way to detect radioactive sources at border crossings. The objective of this research is to

develop a method for identifying the location of a radioactive source using a distributed array of detectors.

For this work, detector measurements and information about the geometry and material properties of the vehicles will be used to triangulate the position of the source. If a source is detected, cameras installed at the border gates will take a picture of each lane of traffic and image recognition software will be used to estimate the types of vehicles (sedan, truck, van, etc.) in each position. Preconstructed cross section models for each type of vehicle will be used to make a cross section model of the entire system. This model will be used in an inverse calculation to determine the expected location of the source. That source location is used with the cross section model in a forward calculation to determine the expected detector signals. If the actual and expected detector measurements are equal, then the source position has been identified. If they are not equal, then the process is iterated. The solution method is outlined in Fig. 1.

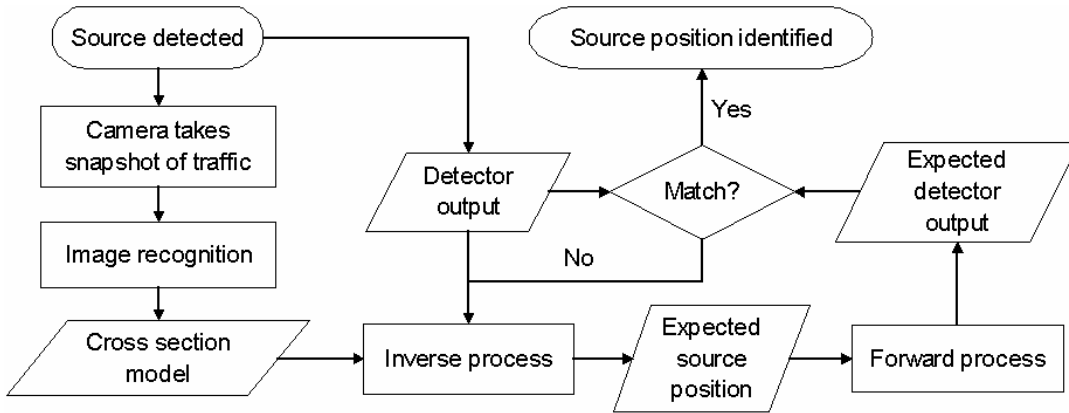


Fig. 1: General solution method for locating radiation sources.

All of the steps on the left column of Fig. 1 are outside the scope of this paper. The following sections assume a known cross section model and detector output. The discussion includes the work that has been done on the forward and inverse processes.

2. Theory

Inverse theory is the set of methods used to extract useful inferences about the world from physical measurements². Extensive research has been done on inverse transport problems for determining material properties of a system³⁻⁶. This work uses some of the same principles for determining the location of a source.

The forward process solves the neutron transport equation with inhomogeneous source Q given by

$$\underline{\Omega} \cdot \nabla \Psi(r, \underline{\Omega}) + \sigma_t(r) \Psi(r, \underline{\Omega}) - \frac{\sigma_s(r)}{4\pi} \int_{4\pi} d\Omega' \Psi(r, \underline{\Omega}') = Q(r, \underline{\Omega}). \quad (1)$$

For brevity this is written as

$$L\Psi = Q, \quad (2)$$

where L is the transport operator defined by Eq. (1). The adjoint transport equation is

$$-\underline{\Omega} \cdot \nabla \Psi^*(r, \underline{\Omega}) + \sigma_t(r) \Psi^*(r, \underline{\Omega}) - \frac{\sigma_s(r)}{4\pi} \int_{4\pi} d\Omega' \Psi^*(r, \underline{\Omega}') = Q^*(r, \underline{\Omega}), \quad (3)$$

which can be shortened to

$$L^* \Psi^* = Q^*. \quad (4)$$

The adjoint source is defined as the difference between the calculated and actual detector response. It is given by

$$Q^* = \sigma_d (\Psi_{\text{det}} - \Psi), \quad (5)$$

where the cross section of the detectors is $\sigma_d(\underline{r}) = \sum_{n=1}^N R_n \delta(\underline{r} - \underline{r}_n)$, for N detectors. Assuming vacuum boundary conditions, the duality principle reads⁷

$$\int_V d^3r \int_{4\pi} d\Omega \Psi^* L \Psi = \int_V d^3r \int_{4\pi} d\Omega \Psi L^* \Psi^*. \quad (6)$$

If the system parameters, such as cross sections or source position, are perturbed, then there will be a change in the flux. Using the chain rule, the change in the transport equation is given by

$$\delta L \Psi + L \delta \Psi = \delta Q, \text{ or}$$

$$L \delta \Psi = \delta Q - \delta L \Psi. \quad (7)$$

The error in the detector response calculated with the forward equation with respect to the actual detector response can be described with a chi-squared error functional:

$$\mathcal{E} = \frac{1}{2} \int_V d^3r \int_{4\pi} d\Omega \sigma_d (\Psi_{\text{det}} - \Psi)^2. \quad (8)$$

The steepest descent method can be used to minimize the error functional⁸. To use this method, the gradient of the error functional with respect to the quantities of interest is needed. For example, the functional gradient (or Fréchet derivative) of the chi-squared error with respect to the x-position is given by

$$\nabla_x \mathcal{E} = \int_V d^3r \int_{4\pi} d\Omega \frac{\partial \Psi}{\partial x} \sigma_d (\Psi_{\text{det}} - \Psi). \quad (9)$$

Using the Eq.'s (4) and (5) to replace the adjoint source and the principle of duality given by Eq. (6), this can be rewritten as

$$\nabla_x \mathcal{E} = \int_V dV \int_{4\pi} d\Omega \Psi^* L \frac{\partial \Psi}{\partial x}. \quad (10)$$

Replace the $L \frac{\partial \Psi}{\partial x}$ term using Eq. (7):

$$\nabla_x \mathcal{E} = \int_V dV \int_{4\pi} d\Omega \Psi^* \left(\frac{\partial Q}{\partial x} - \Psi \frac{\partial L}{\partial x} \right). \quad (11)$$

For the source location problem we assume that all of the cross sections are known, so $\partial L/\partial x = 0$. Also, the source is assumed to be a point source with strength q . Showing the source explicitly for a two-dimensional problem with x - y geometry, Eq. (11) becomes

$$\nabla_x \mathcal{E} = \int_V dV \int_{4\pi} d\Omega \Psi^* \frac{\partial}{\partial x} [q \delta(x - x_0) \delta(y - y_0)], \quad (12)$$

where (x_0, y_0) is the source position. To evaluate this integral, integrate by parts using

$$\int_{x_0-\varepsilon}^{x_0+\varepsilon} dx \frac{d}{dx} [\delta(x - x_0)] f(x) = - \left. \frac{df(x)}{dx} \right|_{x=x_0}. \quad (13)$$

Thus, the functional gradient of the chi-squared error with respect to the x -position is

$$\nabla_x \mathcal{E} = -q \left. \frac{\partial \Phi^*(x, y_0)}{\partial x} \right|_{x=x_0}, \quad (14)$$

where Φ^* is the adjoint scalar flux. The functional gradients of the chi-squared error with respect to the y -position and source strength are found similarly. They are

$$\nabla_y \mathcal{E} = -q \left. \frac{\partial \Phi^*(x_0, y)}{\partial y} \right|_{y=y_0}, \quad (15)$$

$$\nabla_q \mathcal{E} = \Phi^*(x_0, y_0). \quad (16)$$

In a steepest descent algorithm, each iteration updates the quantity of interest by some step size in the direction of steepest descent, which is the negative of the functional gradient. The step size can be calculated in several different ways. For the test problems in the following section, a 1D line search was used to determine the step size.

3. Test Problems

Test problems were run to look at two aspects of the algorithm: (1) the dependence of the solution on the initial guess for source position and (2) how error in the detector measurements affects the solution. Both test problems were run using the same two-dimensional system with x - y geometry. The neutron transport and adjoint equations were solved using a step-difference approximation and an S_{12} quadrature set⁹.

The test system was created to model a simplified-real-world scenario with two lanes of traffic and three detectors. Fig. 2 shows the system layout. The grey boxes are homogeneous—all with the same cross sections—and meant to represent vehicles. The dotted area between the “vehicles” is representative of air space. The detectors are the darker-grey circles. The configuration of the detectors is consistent with actual border crossings. The black square shows the source position. For both test problems the source strength was assumed known, so the algorithm identified source position only.

3.1. Initial Guess Test Problem

For this test the algorithm was run once for each cell in the two-dimensional grid. Each cell was tested as the initial guess for the source position. The objective of the test was to examine how the initial guess affects the solution. Fig. 3 shows that the algorithm estimated that the source is at five different

locations, depending on the initial guess. Outlines of the vehicles and detectors are included in Fig. 3 for reference.

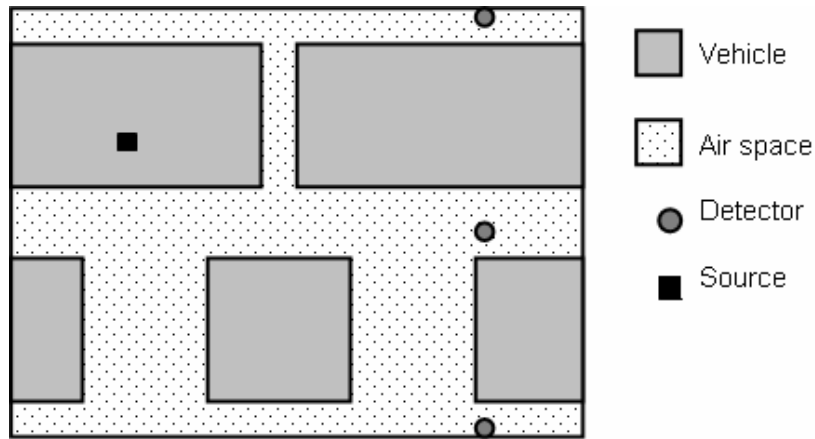


Fig. 2: Layout of the system for the test problems.

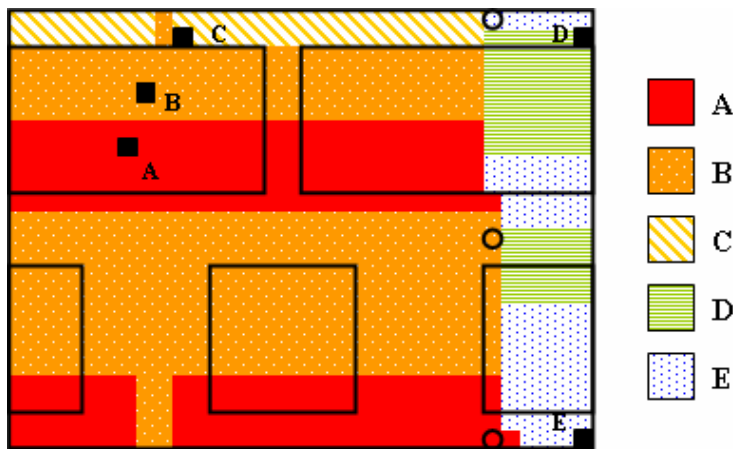


Fig. 3: Estimated source position based on the position of the initial guess.

The estimated source locations are marked in Fig. 3 with a black square and a corresponding letter. Point A is the actual source location. The key for Fig. 3 shows the shading that corresponds to each of the five estimated source locations. For example, all of the cells shaded in solid red converged to point A when those cells were used as the initial guess.

Fig. 3 shows that using most of the cells in the system as the initial guess resulted in either the correct source position being identified (point A) or a point inside the correct vehicle being identified (point B). Using the cells towards the top of the system and to the left of the detectors as the initial guess resulted in point C being identified as the source location in most cases. Point C is just outside of the vehicle that contains the source.

The reason that the solution converged to different positions has to do with the method for minimizing the error functional. As the name implies, the steepest descent method pushes the guess along the path of steepest descent. If that path falls into a local minimum, the steepest descent method will not push the solution out of the local minimum. All of the points estimated as the source location are local minima, and point A is the global minimum.

Using cells to the right of the detectors as the initial guess resulted in the estimated source location being at the right boundary of the system (points D and E). Points D and E are clearly not even close

to the actual source position; however, this result is not surprising. Points D and E are a result of the steepest descent method combined with the configuration of the detectors. Starting with cells to the right of the detectors, the steepest descent algorithm pushed the initial guess on a path away from the detectors. Because the detectors are in line with each other vertically, the difference between the calculated and actual detector readings would have gotten larger (maximizing the error functional) if the source was pushed to the left. If the detectors had been staggered vertically or if there were more detectors towards the left side of the system, the steepest descent method may have pushed the solution in the correct direction.

3.2. Detector Error Test Problem

The second test problem examines the affect of error in the detector measurements on the solution. The same two-dimensional system was used for this test as was used in the first test. The first test assumed that the detector measurements were perfect. Here, the same initial guess was used for all of the tests, but the error in the detector measurements was varied from 0% to 100% in increments of 5%. The initial guess was a cell located near the bottom detector, and it converged to the actual source position when there was 0% error in the detector measurements.

The error in the detector measurements was sampled from a Gaussian distribution, and it was assumed that all three detector measurements were increased by the same average percent error. The distance between the actual source position and the calculated source position divided by the length (in the x-direction) of the system as a function of the error in the detectors is plotted in Fig. 4.

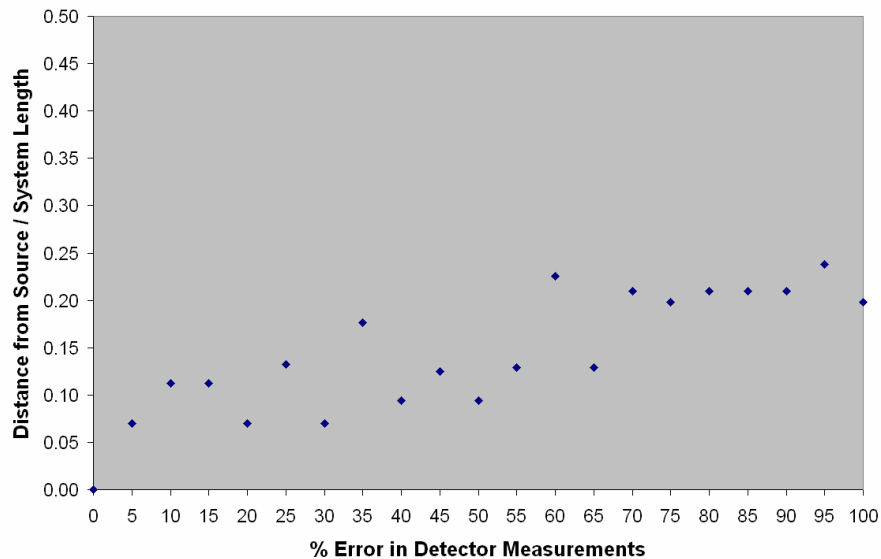


Fig. 4: Distance of the estimated source position from the actual source position divided by the system length as a function of error in the detector measurements.

The plot shows that increasing the error in the detectors caused the predicted source position to move away from the actual source position. For example, 10% error in the detector measurements caused the predicted source position to be a distance approximately 12% of the length of the system away from the actual source position. When the detector error was increased to 80%, the predicted source position was a distance approximately 20% of the system length away from the actual source position.

It is difficult to tell how these results will scale in a larger, more realistic problem with more heterogeneities and detectors that contain error in differing percentages without further testing. The conclusion that can be drawn from this test is that error in the detectors may be a significant factor in how well the algorithm predicts the source location and will need to be considered as this research progresses.

4. Conclusion

An algorithm for identifying the location of a radioactive source using a distributed array of detectors has been developed using forward and adjoint transport equation solutions. It uses the steepest descent method to minimize an error functional that describes the difference between the actual and calculated detector response. Results have shown that the solution is dependent on the initial guess used in the steepest descent algorithm. Also, error in the detector measurements may be an important factor in locating the source position. More study is needed to determine the extent to which detector error affects the solution.

Future work will include improvement of the source location algorithm within the framework of detector error. Other minimization techniques, such as using the conjugate gradient method instead of the steepest descent method, will be tested. Additionally, radiation transport will be included because many of the portal monitors in use detect neutron and gamma radiation, and we will include a method for determining the source strength.

5. References

- [1] United States Government Accountability Office; *GAO-07-133R DNDO's Cost-Benefit Analysis*. Washington, DC; 2006; p 1-11.
- [2] Menke W; *Geophysical Data Analysis: Discrete Inverse Theory*; International Geophysics Series, vol. 45. Academic Press Inc.; U.S.; 1989.
- [3] Norton SJ; *A General Nonlinear Inverse Transport Algorithm Using Forward and Adjoint Flux Computations*; *IEEE Trans. Nucl. Sci.*, vol. 44, no. 2; 1997; p 153-162.
- [4] Larson EW; *Solution of Multidimensional Inverse Transport Problems*; *Journ. Math. Phys.*, vol. 25, no. 1. 1984; p 131-135.
- [5] Favorite JA, Sanchez R; *An Inverse Method for Radiation Transport*; *Radiation Protection Dosimetry*, vol. 116, no 1-4. 2005; p 482-485.
- [6] Klose AD, Hielscher AH; *Optical Tomography Using the Time-Independent Equation of Radiative Transfer—Part 2: Inverse Model*; *Journ. Quant. Spectrosc. & Rad. Trans.*, vol. 72. 2002; p 715-732.
- [7] Ragusa J; *Application of Duality Principles to Solve Inverse Particle Transport Problems: A Framework*. *Trans. Am. Nucl. Soc.*, vol. 93. 2005; p 427-429.
- [8] Burden RL, Faires JD; *Numerical Analysis 7th ed*. Brooks/Cole; U.S.; 2001.
- [9] Lewis EE, Miller WF; *Computational Methods of Neutron Transport*; American Nuclear Society Inc.; La Grange Park, Illinois; 1993.